

Ligand efficiency based approach for efficient virtual screening of compound libraries

Yi-Yu Ke^{a,*}, Mohane Selvaraj Coumar^b, Hui-Yi Shiao^a, Wen-Chieh Wang^a, Chieh-Wen Chen^a,
Jen-Shin Song^a, Chun-Hwa Chen^a, Wen-Hsing Lin^a, Szu-Huei Wu^a, John T. A. Hsu^a, Chung-
Ming Chang^a, Hsing-Pang Hsieh^{a,*}

^a Institute of Biotechnology and Pharmaceutical Research, National Health Research
Institutes, 35 Keyan Road, Zhunan, Miaoli County 350, Taiwan, ROC.

^b Centre for Bioinformatics, School of Life Sciences, Pondicherry University, Kalapet,
Puducherry 605014, India

* Corresponding author: phone: +886-37-246-166 ext. 35708; fax: +886-37-586-456; e-mail:

yyuke@nhri.org.tw, hphsieh@nhri.org.tw.

Abstract

Here we report for the first time the use of fit quality (FQ), a ligand efficiency (LE) based measure for virtual screening (VS) of compound libraries. The LE based VS protocol was used to screen an in-house database of 125,000 compounds to identify aurora kinase A inhibitors. First, 20 known aurora kinase inhibitors were docked to aurora kinase A crystal structure (PDB ID: 2W1C); and the conformations of docked ligand were used to create a pharmacophore (PH) model. The PH model was used to screen the database compounds, and rank (PH rank) them based on the predicted IC_{50} values. Next, LE_Scale, a weight-dependant LE function, was derived from 294 known aurora kinase inhibitors. Using the fit quality (FQ = LE/LE_Scale) score derived from the LE_Scale function, the database compounds were reranked (PH_FQ rank) and the top 151 (0.12% of database) compounds were assessed for aurora kinase A inhibition biochemically. This VS protocol led to the identification of 7 novel hits, with compound **5** showing aurora kinase A IC_{50} = 1.29 μ M. Furthermore, testing of **5** against a panel of 31 kinase reveals that it is selective toward aurora kinase A & B, with < 50% inhibition for other kinases at 10 μ M concentrations and is a suitable candidate for further development. Incorporation of FQ score in the VS protocol not only helped identify a novel aurora kinase inhibitor, **5**, but also increased the hit rate of the VS protocol by improving the enrichment factor (EF) for FQ based screening (EF = 828), compared to PH based screening (EF = 237) alone. The LE based VS protocol disclosed here could be applied

to other targets for hit identification in an efficient manner.

Keywords: Ligand efficiency, Fit quality, Virtual screening, Pharmacophore model, Aurora

kinase inhibitor

1. Introduction

Using the advancements in parallel synthesis technology of the late 1980s and early 1990s, several pharmaceutical companies set up high-throughput screening (HTS) of large compound libraries in order to identify leads for drug development. One of the main disadvantages of HTS is the need to screen a large collection of compounds, which is both time and resource intensive. Recently, virtual screening (VS) is routinely used as a supplement to or as a replacement for HTS in lead identification, due to virtual screening's savings in time and money. VS is a computational method used to score and prioritize HTS library compounds for further biochemical testing [1, 2]. Use of VS can increase the hit rates of lead identification, with some studies reporting hit rates ten times greater or more for VS compared to HTS [3].

Several success stories of lead identification using VS are reported in the literature [3, 4], using either structure-based virtual screening (SBVS) [5] or ligand-based virtual screening (LBVS) [6]. In SBVS, molecular docking of the compounds with the target protein is performed and a score is assigned based on the interaction of the target protein and the compounds; the score of the compounds is used to rank and prioritize them for testing. However, current docking methods have deficiencies in both correctly identifying the crystallographic conformation of the ligands and also accurately scoring the docked poses [7-9]. More critically, availability of target protein information (either 3D X-ray

crystallographic/NMR solved structure or amino acid sequence of the target protein) is essential for SBVS. Hence, in the absence of such protein information, LBVS (an alternative method for VS) is used to identify leads for drug-development projects.

In LBVS, ligand similarities based on either 2D or 3D information of known ligands are used to identify new leads [6]. Particularly, 3D-QSAR (quantitative structure-activity relationship) based techniques — such as CoMFA (comparative molecular field analysis) [10], [11], CoMSIA (comparative molecular similarity indices) [12], and pharmacophore models [13] — are currently much used. A pharmacophore model represents the relative orientation of the functional groups of a molecule in three-dimensional space, which are necessary for maintaining the activity. A typical pharmacophore model constitutes various pharmacophoric elements such as the hydrogen bond acceptor (HBA), hydrogen bond donor (HBD), hydrophobic (HY) group, and excluded volume (EV); the relative positions of the pharmacophoric elements in the model are defined by the distances and angles between them. Pharmacophore models can be generated from a set of known active ligands, by superimposition of the bioactive conformation of the ligands. Recently, several groups have reported the use of pharmacophore models for carrying out VS to identify hits [13].

Hits identified from VS, either from SBVS or LBVS methods, are used as a starting point for lead optimization in drug discovery programs. Retrospective analysis of the starting lead – drug pairs from several successful drug discovery programs reveals that the molecular

properties (molecular weight and lipophilicity) inflation is very common during lead optimization; hence there is a need to keep tight control over them during the process of drug evolution [14]. Moreover, the success of developing a drug depends heavily on the nature of the starting hits chosen for lead optimization. Simple criteria such as activity alone are insufficient for selecting an appropriate hit for optimization; additional criteria such as Ligand efficiency (LE) need to be considered to select the right hit candidates for further optimization [15, 16]. LE can be defined as the binding affinity per heavy atom of the molecule and can be computed from experimental or calculated binding affinity divided by the number of heavy atoms. LE was first introduced in the field of fragment-based drug discovery (FBDD) to select the best of two fragments and is now routinely used to choose the optimized leads during hit to drug evolution in drug discovery programs [17]. It should also be noted that the application of LE has its own limitation as it considers all heavy atoms the same even though oxygen, nitrogen, and other important heavy atoms present in drugs have different physico-chemical and binding properties. This limitation of LE is recognized in the field of drug design; accordingly, the use of the LE function in conjunction with other parameters such as LLE (lipophilic ligand efficiency) during hit selection/optimization in drug discovery programs is recommended [18-20].

The aim of this work is to develop an efficient VS protocol for the improved identification of hits from an HTS library; the VS protocol is exemplified by aurora kinase

inhibitor identification. For this purpose, 125,000 compounds in an in-house HTS library were prioritized for biochemical screening using a two-step procedure (Scheme 1). First, HTS compounds were screened by a pharmacophore model developed using two sets of aurora kinase inhibitors (pyrazoles & furanopyrimidines). The model predicts the IC_{50} of the HTS compounds by matching them to the pharmacophore features of the model and ranks (PH_rank) them based on their predicted activity. In the second step, compounds identified using the pharmacophore model were reranked (PH_FQ rank) using Fit quality (FQ) score, a LE based function. Finally, the top ranked compounds were subjected to biochemical testing for aurora kinase A inhibition. The VS protocol reported here has led to the identification of a potent aurora kinase A inhibitor with an $IC_{50} = 1.29 \mu M$, by testing only 151 compounds from a HTS library of 125,000 compounds. Moreover, incorporation of a LE based scoring function into the VS method has improved the hit rate; such a protocol could be applied to other targets as well.

2. Chemistry

The aurora kinase inhibitor **5** identified in this study was synthesized from commercially available methyl-5-formyl-2-hydroxybenzoate (**8**) and *p*-nitro-aniline (**14**) using a convergent synthesis protocol as shown in Scheme 2. For this purpose, aldehyde **8** was subjected to bromination under acid condition, as reported earlier, to give **9** in quantitative yield [21]. Treatment of **9** with the Grignard reagent – 2-chlorophenylmagnesium bromide in THF at 0°

C provided the secondary alcohol **10** in 65% yield. Acid mediated dehydroxylation of **10** followed by LAH reduction resulted in the primary alcohol **12** in 83% yields, over two steps. The key aldehyde intermediate **13** was prepared from **12** by MnO₂ oxidation, in 77% yield. Next, the aniline intermediate **16** was synthesized from the aniline **14**, by first coupling with 2-furoyl chloride under basic condition to give **15** in 74% yield, followed by hydrogenolysis under H₂ atmosphere over 10% Pd/C in 95% yield. Finally, both intermediates, **13** and **16**, were condensed under reflux conditions to give the desired compound **5** in 52% yield.

3. Results and Discussion

3.1. Pharmacophore model generation and validation

As a first step, we set out to develop an LBVS platform using pharmacophore model for screening the in-house HTS library to identify aurora kinase inhibitors. It is known that 3D pharmacophore based VS is much faster than SBVS. Moreover, pharmacophore-based VS results in the identification of much more diverse chemotypes and is more useful in scaffold-hopping [13]. Albeit these advantages of LBVS, use of SBVS is often much higher than the use of LBVS (pharmacophore) methods for hit identification, due to certain limitations [4]. For instance, the accuracy of the pharmacophore model generated from a set of known active ligands depends on the ability of the algorithm to correctly predict the bioactive conformation of the ligands and then align them. Previous studies by several groups have shown that the docking-based alignment of ligands can overcome this shortcoming and has resulted in better

3D-QSAR models [22, 23]. Hence, in our studies we first planned to use structure-based docking to generate the bioactive conformations of the ligands for alignment and subsequently use them for pharmacophore model building.

The aurora kinase inhibitors used for developing the pharmacophore model were the pyrazole and furanopyrimidine analogs reported by us earlier (Figure 1A) [24-27]. Selection of training and test set compounds (Table S1 and S2, supplemental information) were performed using the Discovery Studio/Cluster Ligands program, as described before for the construction of COMFA and COMSIA 3D-QSAR models [27]. Pharmacophore hypothesis generation was performed by the HypoGen module of Discovery Studio automatically, based on the structure-based alignment derived from docked conformations of 20 training set ligands to the aurora kinase A crystal structure (PDB ID: 2W1C). A total of 20 hypotheses were generated by the HypoGen; the top 10 hypothesis with their statistical parameters and features are shown in Table S3, supplemental information. The quality of pharmacophore hypothesis can be evaluated using various cost functions: total cost, fixed cost, null cost, configuration cost, and error cost [28]. Even though the top three hypothesis (Hypo 1, 2 and 3) have higher correlation values, these three models do not have the important hydrophobic feature corresponding to the back pocket region of the protein (Figure S1, supplemental information). Hydrophobic interaction in the back pocket region of Aurora kinase was identified as essential feature for maintaining potent Aurora kinase inhibition activity in our

previous studies [24-27]. Hence, the hypothesis 4 (Hypo 4) was chosen as the best, with its total cost of 80.00, fixed cost of 51.80, null cost of 165.72, error cost of 70.56, RMS of 1.71, correlation of 0.88, and configuration cost of 7.19. This hypothesis has 90% statistical significance, since the cost differences (Δ Cost) between null and fixed or null and total cost were both greater than 60, implying that hypothesis 4 has a greater than a 90% chance of representing a true correlation between the pharmacophoric features represented by the hypothesis and the aurora kinase A activity. Moreover, the configuration cost of the top hypothesis generated was smaller than 17, which indicates that the hypothesis was not generated by chance and is unlikely to correlate with others.

To further confirm that the hypothesis generated was not by chance correlation, Fischer's randomization test with 95% confidence level was carried out by randomly assigning the activities to the training set molecules. A total of 19 spreadsheets were generated from the randomization of data, but none of them showed statistically significant correlation with the activity data, further confirming that hypothesis 4 is a genuine model (Table S4, supplemental information).

In our previous studies [24-26], both the pyrazole and furanopyrimidine aurora kinase A inhibitors (training set) were found to have the following major structural features that are essential for interaction at the binding site of the enzyme: 1) the N1 nitrogen of furanopyrimidine or pyrazole ring makes hydrogen bond with the protein, 2) the urea side

chain CO group of furanopyrimidine makes another hydrogen bond with the protein, and 3) the urea side chain terminal phenyl group makes hydrophobic interaction in the back pocket. These structural requirements for interaction with aurora kinase A match well with the pharmacophoric features of hypothesis 4 generated by HypoGen (Figure 1B), which includes one hydrogen bond acceptor (HBA), one hydrogen bond donor (HBD), and three hydrophobic features (HY1-HY3).

Next, the prediction ability of this pharmacophore model (Hypothesis 4) was evaluated by the goodness of prediction of aurora kinase A activity for a set of 46 test set compounds (Test set - 1: pyrazoles and furanopyrimidines, Table S2, supplemental information) and 9 aurora kinase inhibitors in clinical trials (Test set - 2: AT9283 - Phase I [29], AZD-1152 - Phase I [30], GSK-1070916 - Phase I [31], MLN-8237 - Phase II [32], PF-03814735 - Phase I [33], PHA-680632 – Preclinical [34], PHA-739358 - Phase II [35], SNS-314 - Phase I [36], and ZM-447439 - Phase I [37], Table S5, supplemental information). The linear regression coefficient for the activity prediction (r_{pred}^2) by the Hypo 4 model for test set-1 and test set-2 were calculated and found to be 0.93 and 0.61, respectively. The r_{pred}^2 value (0.93) of test set-1 is higher than the correlation value (0.88) of the training set for hypothesis 4. This was due to the presence of an outlier compound **37** in the test set-1, which had an IC_{50} of 10,478 nM. This value is over the maximum predictive ability of the training set; the maximum IC_{50} of the training set compound was 7060 nM (for compound **20**). When

the outlier compound **37** was removed, the r^2_{pred} value of test set-1 by Hypo 4 decreased to 0.86. Also the predictive value of Hypo 1, 2, and 3 for test set-1 was calculated as 0.61, 0.46 and 0.37, respectively (Table S6, supplemental information), which was much lower than that of Hypo 4. These results suggest that the model Hypo 4 is able to predict the aurora kinase A inhibitory potential of both the training set related as well as unrelated compounds, with reasonable accuracy.

3.2. Development & validation of ligand efficiency based virtual screening strategy

In the second step, the pharmacophore model was used to screen in-house HTS library of 125,000 compounds to identify novel aurora kinase inhibitors. This could be accomplished by predicting the aurora kinase A activity (IC_{50}) and then ranking (PH rank) the database compounds using the model Hypo 4 and then selecting the top ranked compounds for biochemical testing. In spite of several successful examples of hits identified from VS methods, people are still working to improve the hit rate of VS in order to identify hits cost and resource efficiently. Hit rates refer to the percent of positive hits identified during a database screening campaign; this varies widely, depending upon several factors, including the screening method (SBVS or LBVS) and database used (general library or focused library). Our aim is to efficiently identify aurora kinase lead compounds from a database by utilizing a LE based VS platform.

For this purpose we planned to use ligand efficiency (LE) along with the

pharmacophore based scoring, so as to identify aurora kinase inhibitors more efficiently. Many groups have now used LE metrics to assess hits from VS as well as use the metrics for optimizing hits in drug discovery programs [3, 16]. The LE metric was first defined by Andrews et al. [16], which defines it as biological activity per molecular size ($\frac{\Delta G}{HA}$ or $\frac{pIC_{50}}{HA}$; where ΔG = free energy of binding, HA = number of non hydrogen heavy atoms). Although LE is currently an useful tool in fragment-based drug design (FBDD), it cannot be solely used to judge the better of two fragments with disparate size, since the LE range varies depending on the molecular size of the fragments under consideration [38]. In order to overcome the drawbacks of the LE function and also as an improvement to LE, Reynolds et al., compared more than 8000 ligands and their 28 protein targets and defined a new function, the “fit quality” (FQ) score, to remove the weight dependent problem of ligand efficiency [39]. The fit quality (FQ) score can be defined as size normalized LE metric and can be calculated from the following equation (1):

$$FQ = \frac{LE}{LE_Scale} \quad (1)$$

where LE is the ligand efficiency and LE_Scale is derived from the top ligand efficiency versus heavy atom count curve. Moreover, different types of targets will have different LE_Scale distributions. Hence, to use FQ as a part of the VS scoring function, the LE_Scale for aurora kinase A target needs to be calculated over a range of heavy atom counts. So a diverse set of aurora kinase inhibitors were collected and used to generate the LE_Scale

function based on these compounds.

This diverse set contains 234 known aurora kinase inhibitors with seven different cores (Group 1-7) [40] and 9 aurora kinase inhibitors in clinical trials [29-37] (total 243 control compounds with aurora kinase A IC₅₀ ranging from 1 to 17,219 nM and HA count ranging from 16 to 55). The data (IC₅₀ or K_i values) were collected from literature and their LE (pIC₅₀/HA or pK_i/HA) were calculated (Table S7, supplemental information). In order to derive the LE_Scale, the plot of LE against HA count was generated for all the 243 aurora kinase inhibitors (Figure 2). The LE_scale function was derived by fitting a curve to the highest LE value over the whole range of HA count using OriginPro 7.0 software (OriginLab, Northampton, MA). The equation (2) describes the fitted curve representing the LE_Scale for aurora kinase A target.

$$\text{LE_Scale} = 0.86824 - (0.0563) * \text{HA} + 0.00237 * \text{HA}^2 - (498971\text{E-}5) * \text{HA}^3 + (38647\text{E-}7) * \text{HA}^4 \quad (2)$$

Once LE_Scale function was derived over a range of HA count for the aurora kinase A target, database compounds identified by the pharmacophore model (PH rank) could be FQ scored using equation -1 and reranked (PH_FQ rank). Based on the PH_FQ rank order, compounds could be biochemically tested for their aurora kinase A inhibition. However, randomly choosing the top 100 or 200 compounds from PH_FQ screening may not give optimal results. Hence, to identify the optimal screening threshold point, we planned to calculate the enrichment factor (EF) at different screening threshold points based on the

recovery of 243 known aurora kinase inhibitors from the database by both PH and PH_FQ ranking.

Applying the above strategy, 125,243 compounds (125,000 database + 243 control compounds), were subjected to pharmacophore screening. Out of those, only 894 compounds could be matched to the pharmacophore feature of Hypo 4, with a maximum of 2 features omitted. Based on the predicted IC₅₀ values, these compounds were ranked (PH rank). Then, LE values were calculated using the predicted IC₅₀ for the 894 compounds and the LE_Scale value for their HA count derived from equation (2). FQ values were computed for these compounds from the LE and LE_Scale values using equation (1). Based on the FQ values, these 894 compounds were reranked (PH_FQ rank). All 894 compound codes, along with their predicted IC₅₀, LE, LE_Scale, PH rank, and PH_FQ rank, are shown in Table S8, supplemental information.

Next, the enrichment factor (EF) for the screening was calculated based on the retrieval of control compounds from the database using the equation (3) [41], at different screening threshold levels of 1 to 30%:

$$EF^{x\%} = \frac{Hits_{selected}^{x\%}/N_{selected}^{x\%}}{Hits_{total}/N_{total}} \quad (3)$$

where Hits_{selected}^{x%} is the number of active ligands present in the top x% of the database, Hits_{total} is the total active ligands in the database, N_{selected}^{x%} is number of the compounds in the top x% of the database, N_{total} is number of compounds in the entire

database. $EF^{1\%}$ means enrichment of hits obtained if the top 1% of the database is screened. A random screening of the database would give an $EF^{1\%} = 1$ at the 1% threshold level. Even if the VS protocol can improve EF by a few fold, the method could be considered to be good since the chance of identifying a hit is improved, compared to random screening.

EF for both PH and PH_FQ screening methods at different threshold levels of screening are shown for control compounds in Figure 3A and in Table S9, supplemental information. It shows that incorporation of LE based scoring into the screening protocol improves the hit identification rate (higher EF) at all levels of screening threshold, compared to PH based screening alone. For example, at a screening threshold of 25%, EF for PH based screening is only 2.61; while for PH_FQ based screening EF is 3.48 (Table S9, supplemental information). As maximum EF for PH_FQ based screening was observed at the 25% screening threshold, it was chosen as the threshold point for selecting database compounds for biochemical testing.

To further confirm that PH_FQ based ranking would improve the chance of identifying the hits better than just using PH based ranking, we analyzed the retrieval of control compounds by both methods using receiver operating characteristic (ROC) curve [41, 42]. ROC curve helps to judge the performance of a binary classifier system and provides tools to select optimal models and to discard suboptimal ones. ROC curve was constructed by plotting a graph of sensitivity (Se, true positive rate) vs. 1-specificity (1-Sp, false positive rate)

for both PH and PH_FQ based screening methods. The measure of Se and Sp are defined as

$$Se = \frac{TP}{TP+FN} \quad (4)$$

$$Sp = \frac{TN}{TN+FP} \quad (5)$$

where TP is the number of correctly identified active ligands (true positives), TN the number of correctly identified inactive ligands (true negatives), FP the number of incorrectly identified active ligands (false positives), and FN the number of incorrectly identified inactive ligands (false negatives). The area under the ROC curve (AUC) is a useful measure of the performance of two different virtual screening approaches. The ideal screening method will have an AUC value of 1, while a random screening method would lead to an AUC value of 0.5. The AUC values of the PH and PH_FQ screening methods are 0.65 and 0.84, respectively (Figure 3B). ROC curve analysis further reiterates that the PH_FQ based screening method is better than PH based screening alone and can improve the chance of identifying aurora kinase inhibitors from the database.

3.3. Virtual screening and hit identification

As a third step, based on the PH_FQ reranking, top 223 compounds (25% screening threshold) out of 894 compounds were selected, out of which 72 were control compounds and remaining 151 were database compounds. The top ranked 151 database compounds were tested at 10 μ M concentration for aurora kinase A inhibition using kinase glow assay (Table S8, supplemental information). Out of the 151 compounds tested, 7 compounds, **1-7** showed

more than 50% inhibition at 10 μ M (Table 1). All seven compounds were subjected to IC₅₀ determination, which showed that **5** has an IC₅₀ of 1.29 μ M. In order to confirm that **5** is a potent aurora kinase A inhibitor and also to assess its overall kinase profile we synthesized the compound as shown in scheme 2 and tested the compound in a panel of 31 kinases at 10 μ M concentration using Life Technologies Corporation, Z-LYTE® screening assay (Table S10, supporting information). The kinase profiling data demonstrate that compound **5** is a potent and selective aurora kinase inhibitor.

Further, the lead **5** identified was docked to aurora kinase A crystal structure (PDB ID: 2W1C) and mapped to pharmacophore Hypo 4, with an aim to understand the protein-ligand interactions (Figure 4). Docking showed that the phenolic OH group acts as a hydrogen bond acceptor (HBA) to interact with the Glu211 residue in the hinge region and the NH group of amide functionality acts as a hydrogen bond donor (HBD) to interact with Glu181 residue in the α C helix. An additional H-bond was observed between the Asp274 of the DFG loop and the amide carbonyl group next to the furan ring. The furan ring maps onto the HY3 hydrophobic region and makes hydrophobic contact with Glu181, Asp274, and Lys162. The two phenyl rings (Cl-Ph- and =N-Ph-NH-) map to the HY1 and HY2 regions of the pharmacophore model and makes extensive contact with the Leu 139, Gly 140, Lys141, Val 147, Lys162, Glu181, Leu210, and Asp274 residues in the ATP binding site.

To confirm that the PH_FQ screening had actually improved the hit rates, the rank

order of active hits in each screening methods can be compared (Table 1). When the screening threshold is set to top 100 compounds, there is 0 hits from PH screening method and 3 hits from PH_FQ screening method. If the screening threshold is set as 214 compounds, PH_FQ screening method would have identified all the 7 hits, but PH screening would have only identified 2 hits. Moreover, comparison of EF for VS method with and without FQ ranking for the identification of control as well as new hits (from database) shows that the VS incorporating FQ based scoring is better in both the cases (Table 2). This further emphasize that incorporation of the LE based metric, FQ, to the pharmacophore based screening had improved the hit rate of VS and helped in identifying a selective aurora kinase inhibitor **5**.

4. Conclusion

Identification of a suitable hit molecule for further optimization to a lead is an important step in the early stages of drug discovery. In this regard, nowadays virtual screening (VS) is extensively used to identify suitable hits and methods to improve the VS hit rate (% of hits identified to compounds tested biochemically) is much sought after. In this study, we report for the first time the use of a ligand efficiency (LE) based metric, – Fit quality (FQ), to rank database compounds and prioritize them for biochemical testing in aurora kinase A inhibition assay.

The in-house database compounds (125,000) were first screened using a pharmacophore model (PH screening) developed using 20 known aurora kinase inhibitors.

Next, LE_Scale function was derived from 294 known aurora kinase inhibitors, which defines the maximum LE achievable for a particular heavy atom count for the aurora kinase target. The LE_scale function was used to calculate the fit quality (FQ) score for PH screened database compounds. Based on the FQ score (PH_FQ screening), the top 151 compounds (0.12% of database) were tested biochemically to identify **5** as a novel aurora kinase selective inhibitor. Incorporating a LE based metric, FQ, into VS clearly improved the enrichment factor (EF) — from 237 (PH screening) to 828 (PH_FQ screening) — indicating that FQ based VS is more efficient method for hit identification. The LE based VS protocol described here for aurora kinase hit identification could be utilized for other drug targets to identify hits more efficiently.

5. Experimental

5.1. Pharmacophore generation

The pyrazole and furanopyrimidine aurora kinase inhibitors reported earlier were assigned to training and test set compounds as described before (Table S1 and S2, supplemental information) [27]. The pharmacophore generation was performed using Discovery Studio/3D-QSAR pharmacophore generation software (Discovery Studio 2.1, Accelrys Inc., San Diego, CA, USA). In the parameter setting, the Uncert value was set to 1.4, due to the narrow range of activities (IC_{50} values of 33–7060 nM) of the compounds. Minimum interfeature distance was set as 2.5 Å, and the maximum excluded volumes were set to 100.

Minimum and maximum pharmacophore features were set as 4 and 5, respectively. Three pharmacophore features were derived by the HypoGen algorithm: hydrogen bond acceptor (HBA), hydrogen bond donor (HBD), and hydrophobic (HY). The quality of the pharmacophore hypothesis constructed was assessed by the Fischer validation, with confidence level of 95%, and was based on Fischer's randomization test by randomly assigning the activities of the training set molecules as new spreadsheets. The prediction ability of the pharmacophore was evaluated by the goodness of prediction of activity for 55 test set aurora kinase inhibitors (Test set - 1: 46 pyrazoles and furanopyrimidines, Table S2, supplemental information + Test set - 2: 9 aurora kinase inhibitors in clinical trials, Table S5, supplemental information). The linear regression coefficient for the activity prediction (r^2_{pred}) was used as a parameter to ascertain the prediction ability of the model.

5.2. *Virtual screening*

The first round of VS was done by using Discovery Studio/ Ligand Pharmacophore Mapping program. The Hypo 4 was used for screening the in-house database (125,243 = 125,000 database + 243 control compounds). The database compound conformations were generated by Discovery Studio/ Conformation program; the "best" method and the conformers were created within the relative energy threshold of 20 kcal/mol. The maximum number of conformations allowed for each compound was set to 300. The conformations generated were used for performing the virtual screening. The screening method used the "best mapping"

with flexible fit between ligand and the pharmacophore. The maximum number of features that are allowed to miss when mapping the ligand to the pharmacophore was set to 2. The minimum distance between ligand and features was set as 2 Å. Pharmacophore based ranking (PH rank) of the database compounds using Hypo 4 resulted in the identification of 894 compounds (811 database + 83 control compounds) from the database. The second run of VS was done by LE based screening. The heavy atoms of the 894 compounds were calculated and used for determining the FQ value of the compounds ($FQ = LE/LE_{scale}$). Finally, the 894 compounds were ranked (PH_FQ rank) by their FQ value and the top 25% (223 = 151 database + 72 control compounds) database compounds sent for biochemical testing.

5.3. *Synthesis of hit 5*

5.3.1. 3-Bromo-5-[(2-chloro-phenyl)-hydroxy-methyl]-2-hydroxy-benzoic acid methyl ester (**10**).

A solution of compound **9** (800 mg, 3.09 mmol) in THF (15 mL) was added to 2-chlorophenylmagnesium bromide (9.27 mmol) in THF (9 mL) and stirred for 2 h under ice bath condition. The reaction was quenched by the addition of saturated NH_4Cl (aq.) (20 mL), followed by extraction with EtOAc (2 × 20 mL). The combined organics were dried over $MgSO_4$ and concentrated under reduced pressure. The residue obtained was purified by flash column chromatography on silica gel (EtOAc/Hexane = 1:4) to furnish compound **10** (741.4 mg, 65%). 1H NMR (400 MHz, $CDCl_3$): δ 11.45 (s, 1H), 7.88 (d, J = 2.0 Hz, 1H), 7.74 (d, J =

2.0 Hz, 1H), 7.58 (d, $J = 7.6$ Hz, 1H), 7.38-7.26 (m, 3H), 6.16 (s, 1H), 3.96 (s, 3H), 2.41 (s, 1H). ^{13}C NMR (100 MHz, CDCl_3): δ 169.7 (C), 157.0 (C), 139.9 (C), 137.1 (CH), 134.1 (C), 131.8 (C), 129.3 (CH), 128.7 (CH), 127.4 (CH), 127.2 (CH), 127.0 (CH), 112.7 (C), 110.9 (C), 70.8 (CH), 52.6 (CH_3). LCMS (ESI) m/z : 394.9 ($\text{M}+\text{Na}$) $^+$.

5.3.2. 3-Bromo-5-(2-chloro-benzyl)-2-hydroxy-benzoic acid methyl ester (**11**).

To a solution of compound **10** (741.4 mg, 2.08 mmol) in CH_2Cl_2 (10 mL), trifluoroacetic acid (1.14 g, 10.00 mmol) and triethylsilane (697.7 mg, 6.00 mmol) were added, and the mixture was stirred for 1 h at room temperature. Then the reaction mixture was concentrated under reduced pressure to furnish compound **11** (615.3 mg, 83%), which was used for the next step without further purification. ^1H NMR (400 MHz, CDCl_3): δ 11.33 (s, 1H), 7.66 (d, $J = 2.4$ Hz, 1H), 7.55 (d, $J = 2.4$ Hz, 1H), 7.39 (d, $J = 6.8$ Hz, 1H), 7.22-7.13 (m, 3H), 4.01 (s, 2H), 3.95 (s, 3H). ^{13}C NMR (100 MHz, CDCl_3): δ 170.1 (C), 156.6 (C), 139.4 (CH), 137.7 (C), 134.1 (C), 131.3 (C), 130.8 (CH), 129.5 (CH), 129.4 (CH), 128.1 (CH), 127.0 (CH), 113.2 (C), 111.2 (C), 52.7 (CH_3), 38.0 (CH_2). LCMS (ESI) m/z : 378.9 ($\text{M}+\text{Na}$) $^+$.

5.3.3. 2-Bromo-4-(2-chloro-benzyl)-6-hydroxymethyl-phenol (**12**).

To a solution of lithium aluminum hydride (124.5 mg, 3.28 mmol) in THF (2 mL) maintained under ice bath condition, a solution of compound **11** (584.5 mg, 1.64 mmol) in THF (2 mL) was added and stirred for 2 h. The reaction was quenched by the addition of saturated Na_2SO_4 (aq.) (0.3 mL) and stirring the mixture for 10 min. Then the mixture was extracted with Et_2O (2

× 20 mL), and the combined organics were washed with H₂O and brine. Then the organics were dried over MgSO₄ and concentrated under reduced pressure to furnish compound **12** (532.5 mg, quant.), which was used for next step without further purification. ¹H NMR (300 MHz, CDCl₃): δ 7.38 (d, *J* = 5.1 Hz, 1H), 7.36 -7.15 (m, 4H), 6.97 (s, 1H), 4.75 (s, 2H), 4.00 (s, 2H). ¹³C NMR (100 MHz, CDCl₃): δ 149.6 (C), 138.1 (C), 134.1 (C), 132.8 (C), 131.9 (CH), 130.9 (CH), 129.7 (CH), 128.2 (CH), 127.9 (CH), 127.1 (C), 127.0 (CH), 110.4 (C), 63.0 (CH₂), 38.0 (CH₂). LCMS (ESI) *m/z*: 350.9 (M+Na)⁺.

5.3.4. 3-Bromo-5-(2-chloro-benzyl)-2-hydroxy-benzaldehyde (**13**).

To a solution of compound **12** (532.5 mg, 1.63 mmol) in CH₂Cl₂ (8 mL) and MeOH (0.8 mL), MnO₂ (1.42 g, 16.3 mmol) was added and stirred for 8 h under room temperature. The mixture was concentrated under reduced pressure and purified by flash column chromatography on silica gel (EtOAc/Hexane = 1:2) to furnish compound **13** (408.1 mg, 77%). ¹H NMR (400 MHz, CDCl₃): δ 11.47 (s, 1H), 9.79 (s, 1H), 7.64 (d, *J* = 2.0 Hz, 1H), 7.41 (d, *J* = 6.4 Hz, 1H), 7.32 (d, *J* = 2.0 Hz, 1H), 7.25-7.19 (m, 3H), 4.08 (s, 2H). ¹³C NMR (100 MHz, CDCl₃): δ 195.8 (CH), 156.3 (C), 140.2 (CH), 140.1 (C), 137.1 (C), 134.0 (CH), 132.6 (C), 130.8 (CH), 129.7 (CH), 128.2 (CH), 127.1 (CH), 120.8 (C), 111.0 (C), 37.7 (CH₂). LCMS (ESI) *m/z*: 348.8 (M+Na)⁺.

5.3.5. Furan-2-carboxylic acid (4-nitro-phenyl)-amide (**15**).

To a solution of 4- nitroaniline (500 mg, 3.62 mmol) and triethylamine (54.9 mg, 0.54 mmol)

in CH₂Cl₂ (18 mL) was added 2-furoyl chloride (472.5 mg, 3.62 mmol), and the mixture was stirred for 8 h at room temperature. After completion of the reaction, the organics were washed with H₂O (2 × 10 mL). The organic layer was dried over MgSO₄ and concentrated under reduced pressure. The residue was purified by flash column chromatography on silica gel (EtOAc/Hexane = 1:3) to furnish compound **15** (622.4 mg, 74%). ¹H NMR (400 MHz, CDCl₃) δ 8.35 (s, 1H), 8.27 (d, *J* = 7.2 Hz, 2H), 7.85 (d, *J* = 7.2 Hz, 2H), 7.57 (d, *J* = 1.6 Hz, 1H), 7.33 (dd, *J* = 3.6, 1H), 6.62 (dd, *J* = 3.6, 1.6 Hz, 1H). ¹³C NMR (75 MHz, CD₃OD): δ 148.3 (C), 147.5 (C), 143.4 (C), 127.1 (CH ×2), 125.8 (CH), 121.4 (C), 119.4 (CH ×2), 117.4 (CH), 113.6 (CH). LCMS (ESI) *m/z*: 255.0 (M+Na)⁺.

5.3.6. Furan-2-carboxylic acid (4-amino-phenyl)-amide (**16**).

A solution of compound **15** (498.9 mg, 2.15 mmol) and 10% Pd/C (50 mg) in EtOH (10 mL) was stirred under hydrogen atmosphere for 8 h. The reaction mixture was filtered over Celite, and the solvents removed by reduced pressure. The residue obtained was purified by flash column chromatography on silica gel (MeOH/CH₂Cl₂ = 1:40) to furnish compound **16** (413.8 mg, 95%). ¹H NMR (300 MHz, CDCl₃) δ 7.92 (s, 1H), 7.49 (dd, *J* = 1.8, 0.9 Hz, 1H), 7.42 (d, *J* = 8.7 Hz, 2H), 7.20 (d, *J* = 3.3 Hz, 1H), 6.69 (d, *J* = 8.7 Hz, 2H), 6.54 (dd, *J* = 3.3, 1.8 Hz, 1H), 3.64 (s, 2H). ¹³C NMR (100 MHz, CDCl₃): δ 155.9 (C), 148.0 (C), 143.9 (CH), 143.5 (C), 128.6 (C), 121.9 (CH ×2), 115.4 (CH ×2), 114.7 (CH). LCMS (APCI) *m/z*: 203.1 (M+H)⁺.

5.3.7. Furan-2-carboxylic acid (4-{[3-bromo-5-(2-chloro-benzyl)-2-hydroxy-benzylidene] - amino}- phenyl)-amide (**5**).

A solution of compound **13** (179.1 mg, 0.55 mmol) and compound **16** (110.7 mg, 0.55 mmol) in EtOH (3 mL) was stirred under reflux for 2 h. The precipitate formed was filtered to furnish compound **5** (145.4 mg, 52%). ¹H NMR (400 MHz, *d*₆-DMSO): δ 10.33 (s, 1H), 8.97 (s, 1H), 7.95 (d, *J* = 1.6 Hz, 1H), 7.85 (d, *J* = 8.8 Hz, 2H), 7.56 (d, *J* = 2.0 Hz, 1H), 7.50 (d, *J* = 8.8 Hz, 2H), 7.46-7.26 (m, 6H), 6.71 (dd, *J* = 3.6, 1.6 Hz, 1H), 4.05 (s, 2H). ¹³C NMR (100 MHz, *d*⁶-DMSO): δ 161.4 (CH), 156.2 (C), 156.0 (C), 147.4 (C), 145.8 (CH), 141.7 (C), 138.2 (C), 138.0 (C), 135.9 (CH), 133.1 (C), 131.9 (CH), 131.4 (CH), 131.1 (C), 129.5 (CH), 128.4 (CH), 127.5 (CH), 122.0 (CH × 2), 121.0 (CH × 2), 119.7 (C), 115.0 (CH), 112.2 (CH), 109.9 (C), 37.0 (CH₂). LCMS (APCI) *m/z*: 511.0 (M+H)⁺.

5.4 Aurora kinase A inhibition assay

Aurora kinase A inhibition assays for the compounds were carried out as described by us previously [43].

Supplementary data

Supplementary data associated with this article can be found in the online version. These data include the training set and test set of the pharmacophore model, statistical parameters and features of the top ten hypotheses, known aurora kinase inhibitors used for deriving FQ, FQ rank calculation, and enrichment factor (EF) calculation, as well as the kinase selectivity

profile of **5** and ^1H NMR and ^{13}C NMR scan of synthesized compounds.

Abbreviations

3D-QSAR: three dimensional quantitative structure-activity relationship, EF: enrichment factor, FBDD: fragment-based drug discovery, FQ: fit quality, HA: number of heavy atoms, HBA: hydrogen bond acceptor, HBD: hydrogen bond donor, HTS: high through-put screening, HY: hydrophobic, LBVS: ligand-based virtual screening, LE: ligand efficiency, PH: pharmacophore model, ROC: receiver operating characteristic, SBVS: structure-based virtual screening, VS: virtual screening.

Acknowledgements

Financial support from the National Health Research Institutes and the National Science Council, Taiwan (NSC-102-2325-B-400-003 and NSC-101-2113-M-400-002-MY4 to HPH; NSC-102-2113-M-400-003-MY3, to HYS), and from the Science & Engineering Research Board, India (SR/FT/LS-64/2011 to MSC), are gratefully acknowledged.

References

- [1] R.V. Guido, G. Oliva, A.D. Andricopulo, Virtual screening and its integration with modern drug design technologies, *Curr. Med. Chem.* 15 (2008) 37–46.
- [2] T. Polgar, G.M. Keseru, Integration of virtual and high throughput screening in lead discovery settings, *Comb. Chem. High Throughput Screen.* 14 (2011) 889–897.
- [3] T. Zhu, S. Cao, P.C. Su, R. Patel, D. Shah, H.B. Chokshi, R. Szukala, M.E. Johnson, K.E. Hevener, Hit identification and optimization in virtual screening: practical recommendations based on a critical literature analysis, *J. Med. Chem.* 56 (2013) 6560–6572.
- [4] P. Ripphausen, B. Nisius, L. Peltason, J. Bajorath, Quo vadis, virtual screening? A comprehensive survey of prospective applications, *J. Med. Chem.* 53 (2010) 8461–8467.
- [5] P. Ripphausen, D. Stumpfe, J. Bajorath, Analysis of structure-based virtual screening studies and characterization of identified active compounds, *Future Med. Chem.* 4 (2012) 603–613.
- [6] P. Ripphausen, B. Nisius, J. Bajorath, State-of-the-art in ligand-based virtual screening, *Drug Discov. Today* 16 (2011) 372–376.
- [7] G.L. Warren, C.W. Andrews, A.M. Capelli, B. Clarke, J. LaLonde, M.H. Lambert, M. Lindvall, N. Nevins, S.F. Semus, S. Senger, G. Tedesco, I.D. Wall, J.M. Woolven, C.E.

- Peishoff, M.S. Head, A critical assessment of docking programs and scoring functions, *J. Med. Chem.* 49 (2006) 5912–5931.
- [8] K. Heikamp, J. Bajorath, The future of virtual compound screening, *Chem. Biol. Drug Des.* 81 (2013) 33–40.
- [9] T. Scior, A. Bender, G. Tresadern, J.L. Medina-Franco, K. Martinez-Mayorga, T. Langer, K. Cuanalo-Contreras, D.K. Agrafiotis, Recognizing pitfalls in virtual screening: a critical review, *J. Chem. Inf. Model.* 52 (2012) 867–881.
- [10] R.D. Cramer, D.E. Patterson, J.D. Bunce, Comparative molecular field analysis (CoMFA). 1. Effect of shape on binding of steroids to carrier proteins, *J. Am. Chem. Soc.* 110 (1988) 5959–5967.
- [11] L. Zhang, K.C. Tsai, L. Du, H. Fang, M. Li, W. Xu, How to generate reliable and predictive CoMFA models, *Curr. Med. Chem.* 18 (2010) 923–930.
- [12] G. Klebe, U. Abraham, T. Mietzner, Molecular similarity indices in a comparative analysis (CoMSIA) of drug molecules to correlate and predict their biological activity, *J. Med. Chem.* 37 (1994) 4130–4146.
- [13] D. Horvath, Pharmacophore-based virtual screening, in: J. Bajorath (Ed.) *Methods Mol. Biol.*, Humana Press 2011, pp. 261–298.
- [14] E. Perola, An analysis of the binding efficiencies of drugs and their leads in successful drug discovery programs, *J. Med. Chem.* 53 (2010) 2986–2997.

- [15] M.M. Hann, G.M. Keseru, Finding the sweet spot: the role of nature and nurture in medicinal chemistry, *Nature Rev. Drug Discov.* 11 (2012) 355–365.
- [16] A.L. Hopkins, C.R. Groom, A. Alex, Ligand efficiency: a useful metric for lead selection, *Drug Discov. Today* 9 (2004) 430–431.
- [17] S.D. Bembenek, B.A. Tounge, C.H. Reynolds, Ligand efficiency and fragment-based drug discovery, *Drug Discov. Today* 14 (2009) 278–283.
- [18] C.W. Murray, D.A. Erlanson, A.L. Hopkins, G.M. Keserü, P.D. Leeson, D.C. Rees, C.H. Reynolds, Validity of ligand efficiency metrics, *ACS Med Chem Lett* (2014) DOI: 10.1021/ml500146d.
- [19] A.L. Hopkins, G.M. Keseru, P.D. Leeson, D.C. Rees, C.H. Reynolds, The role of ligand efficiency metrics in drug discovery, *Nat Rev Drug Discov* 13 (2014) 105–121.
- [20] M.D. Shultz, Setting expectations in molecular optimizations: Strengths and limitations of commonly used composite parameters, *Bioorg Med Chem Lett* 23 (2013) 5980–5991.
- [21] C.M. Timmers, W.F.J. Karstens, P.P.M. Grima, 4-PHENYL-5-OXO-1,4,5,6,7,8-hexahydroquinoline derivatives as medicaments for the treatment of infertility, in, WO2006117370 A1, 2006.
- [22] I. Muegge, B.L. Podlogar, 3D-Quantitative structure activity relationships of biphenyl carboxylic acid MMP-3 inhibitors: exploring automated docking as alignment method,

Quant. Struct.-Act. Relat. 20 (2001) 215–222.

- [23] Y.Y. Ke, T.H. Lin, Modeling the ligand-receptor interaction for a series of inhibitors of the capsid protein of enterovirus 71 using several three-dimensional quantitative structure-activity relationship techniques, *J. Med. Chem.* 49 (2006) 4517–4525.
- [24] M.S. Coumar, C.Y. Chu, C.W. Lin, H.Y. Shiao, Y.L. Ho, R. Reddy, W.H. Lin, C.H. Chen, Y.H. Peng, J.S. Leou, T.W. Lien, C.T. Huang, M.Y. Fang, S.H. Wu, J.S. Wu, S.K. Chittimalla, J.S. Song, J.T. Hsu, S.Y. Wu, C.C. Liao, Y.S. Chao, H.P. Hsieh, Fast-forwarding hit to lead: aurora and epidermal growth factor receptor kinase inhibitor lead identification, *J. Med. Chem.* 53 (2010) 4980–4988.
- [25] M.S. Coumar, M.T. Tsai, C.Y. Chu, B.J. Uang, W.H. Lin, C.Y. Chang, T.Y. Chang, J.S. Leou, C.H. Teng, J.S. Wu, M.Y. Fang, C.H. Chen, J.T. Hsu, S.Y. Wu, Y.S. Chao, H.P. Hsieh, Identification, SAR studies, and X-ray co-crystallographic analysis of a novel furanopyrimidine aurora kinase A inhibitor, *ChemMedChem* 5 (2010) 255–267.
- [26] M.S. Coumar, J.S. Leou, P. Shukla, J.S. Wu, A.K. Dixit, W.H. Lin, C.Y. Chang, T.W. Lien, U.K. Tan, C.H. Chen, J.T. Hsu, Y.S. Chao, S.Y. Wu, H.P. Hsieh, Structure-based drug design of novel Aurora kinase A inhibitors: structural basis for potency and specificity, *J. Med. Chem.* 52 (2009) 1050–1062.
- [27] Y.Y. Ke, H.Y. Shiao, Y.C. Hsu, C.Y. Chu, W.C. Wang, Y.C. Lee, W.H. Lin, C.H. Chen, J.T. Hsu, C.W. Chang, C.W. Lin, T.K. Yeh, Y.S. Chao, M.S. Coumar, H.P. Hsieh, 3D-

- QSAR-assisted drug design: identification of a potent quinazoline-based aurora kinase inhibitor, *ChemMedChem* 8 (2013) 136–148.
- [28] J. Sutter, O.F. Guner, R. Hoffman, H. Li, M. Waldman, Effect of Variable Weight and Tolerances on Predictive Model Generation, in: O.F. Guner (Ed.) *Pharmacophore Perception, Development, and Use in Drug Design*, International University Line, La Jolla, CA, 1999, pp. 501–511.
- [29] S. Howard, V. Berdini, J.A. Boulstridge, M.G. Carr, D.M. Cross, J. Curry, L.A. Devine, T.R. Early, L. Fazal, A.L. Gill, M. Heathcote, S. Maman, J.E. Matthews, R.L. McMenamin, E.F. Navarro, M.A. O'Brien, M. O'Reilly, D.C. Rees, M. Reule, D. Tisi, G. Williams, M. Vinkovic, P.G. Wyatt, Fragment-based discovery of the pyrazol-4-yl urea (AT9283), a multitargeted kinase inhibitor with potent aurora kinase activity, *J. Med. Chem.* 52 (2009) 379–388.
- [30] R.W. Wilkinson, R. Odedra, S.P. Heaton, S.R. Wedge, N.J. Keen, C. Crafter, J.R. Foster, M.C. Brady, A. Bigley, E. Brown, K.F. Byth, N.C. Barrass, K.E. Mundt, K.M. Foote, N.M. Heron, F.H. Jung, A.A. Mortlock, F.T. Boyle, S. Green, AZD1152, a selective inhibitor of Aurora B kinase, inhibits human tumor xenograft growth by inducing apoptosis, *Clin. Cancer Res.* 13 (2007) 3682–3688.
- [31] M.A. Hardwicke, C.A. Oleykowski, R. Plant, J. Wang, Q. Liao, K. Moss, K. Newlander, J.L. Adams, D. Dhanak, J. Yang, Z. Lai, D. Sutton, D. Patrick,

- GSK1070916, a potent Aurora B/C kinase inhibitor with broad antitumor activity in tissue culture cells and human tumor xenograft models, *Mol. Cancer Ther.* 8 (2009) 1808–1817.
- [32] G. Gorgun, E. Calabrese, T. Hideshima, J. Ecsedy, G. Perrone, M. Mani, H. Ikeda, G. Bianchi, Y. Hu, D. Cirstea, L. Santo, Y.T. Tai, S. Nahar, M. Zheng, M. Bandi, R.D. Carrasco, N. Raje, N. Munshi, P. Richardson, K.C. Anderson, A novel Aurora-A kinase inhibitor MLN8237 induces cytotoxicity and cell-cycle arrest in multiple myeloma, *Blood* 115 (2010) 5202–5213.
- [33] J.P. Jani, J. Arcari, V. Bernardo, S.K. Bhattacharya, D. Briere, B.D. Cohen, K. Coleman, J.G. Christensen, E.O. Emerson, A. Jakowski, K. Hook, G. Los, J.D. Moyer, I. Pruijboom-Brees, L. Pustilnik, A.M. Rossi, S.J. Steyn, C. Su, K. Tsaparikos, D. Wishka, K. Yoon, J.L. Jakubczak, PF-03814735, an orally bioavailable small molecule aurora kinase inhibitor for cancer therapy, *Mol. Cancer Ther.* 9 (2010) 883–894.
- [34] C. Soncini, P. Carpinelli, L. Gianellini, D. Fancelli, P. Vianello, L. Rusconi, P. Storici, P. Zugnoni, E. Pesenti, V. Croci, R. Ceruti, M.L. Giorgini, P. Cappella, D. Ballinari, F. Sola, M. Varasi, R. Bravo, J. Moll, PHA-680632, a novel Aurora kinase inhibitor with potent antitumoral activity, *Clin. Cancer Res.* 12 (2006) 4080–4089.
- [35] P. Carpinelli, R. Ceruti, M.L. Giorgini, P. Cappella, L. Gianellini, V. Croci, A.

- Degrassi, G. Texido, M. Rocchetti, P. Vianello, L. Rusconi, P. Storici, P. Zugnoni, C. Arrigoni, C. Soncini, C. Alli, V. Patton, A. Marsiglio, D. Ballinari, E. Pesenti, D. Fancelli, J. Moll, PHA-739358, a potent inhibitor of Aurora kinases with a selective target inhibition profile relevant to cancer, *Mol. Cancer Ther.* 6 (2007) 3158–3168.
- [36] E.C. VanderPorten, P. Taverna, J.N. Hogan, M.D. Ballinger, W.M. Flanagan, R.V. Fucini, The Aurora kinase inhibitor SNS-314 shows broad therapeutic potential with chemotherapeutics and synergy with microtubule-targeted agents in a colon carcinoma model, *Mol. Cancer Ther.* 8 (2009) 930–939.
- [37] Z.J. Long, J. Xu, M. Yan, J.G. Zhang, Z. Guan, D.Z. Xu, X.R. Wang, J. Yao, F.M. Zheng, G.L. Chu, J.X. Cao, Y.X. Zeng, Q. Liu, ZM 447439 inhibition of aurora kinase induces Hep2 cancer cell apoptosis in three-dimensional culture, *Cell Cycle* 7 (2008) 1473–1479.
- [38] C.H. Reynolds, S.D. Bembenek, B.A. Tounge, The role of molecular size in ligand efficiency, *Bioorg. Med. Chem. Lett.* 17 (2007) 4258–4261.
- [39] C.H. Reynolds, B.A. Tounge, S.D. Bembenek, Ligand binding efficiency: trends, physical basis, and implications, *J. Med. Chem.* 51 (2008) 2432–2438.
- [40] H.X. Zhang, Y. Li, X. Wang, Y.H. Wang, Probing the structural requirements of A-type Aurora kinase inhibitors using 3D-QSAR and molecular docking analysis, *J. Mol. Model.* 18 (2012) 1107–1122.

- [41] J.F. Truchon, C.I. Bayly, Evaluating virtual screening methods: good and bad metrics for the "early recognition" problem, *J. Chem. Inf. Model.* 47 (2007) 488–508.
- [42] P. Baldi, S. Brunak, Y. Chauvin, C.A. Andersen, H. Nielsen, Assessing the accuracy of prediction algorithms for classification: an overview, *Bioinformatics* 16 (2000) 412–424.
- [43] H.Y. Shiao, M.S. Coumar, C.W. Chang, Y.Y. Ke, Y.H. Chi, C.Y. Chu, H.Y. Sun, C.H. Chen, W.H. Lin, K.S. Fung, P.C. Kuo, C.T. Huang, K.Y. Chang, C.T. Lu, J.T. Hsu, C.T. Chen, W.T. Jiaang, Y.S. Chao, H.P. Hsieh, Optimization of ligand and lipophilic efficiency to identify an in vivo active furano-pyrimidine aurora kinase inhibitor, *J. Med. Chem.* 56 (2013) 5247–5260.

Figure legends

Figure 1. (A) General structures of known aurora kinase inhibitors (pyrazoles and furanopyrimidines) used for constructing the pharmacophore model (see Table S1 and S2, supplemental information, for details of training and test sets). (B) Alignment of docked conformations (generated by docking to 2W1C crystal structure) of training set compounds with Hypo 4 model. The model contains five features: one hydrogen bond acceptor (HBA, green spheres), one hydrogen bond donor (HBD, magenta spheres), and three hydrophobic features (HY1, HY2, and HY3, cyan spheres).

Figure 2. Derivation of LE_Scale function from the plot of ligand efficiency (LE) vs. heavy atom (HA) count of known aurora kinase inhibitors (Group 1–7) and 9 clinical drugs (total 243 control compounds). The LE_Scale function is represented by a black line, which is fitted to the highest LE values over a range of HA count.

Figure 3. Analysis of control compound retrieval from HTS database. (A) Comparison of enrichment factor (EF) at screening threshold of 1 to 30% for PH and PH_FQ screening methods. (B) Comparison of ROC curve of PH and PH_FQ screening methods.

Figure 4. Docking of hit **5** to aurora kinase A (PDB ID: 2W1C). (A) Mapping of docked

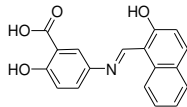
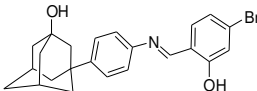
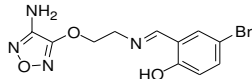
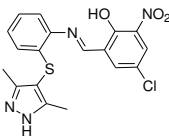
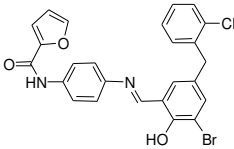
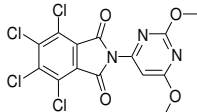
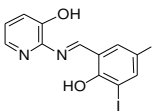
conformation of hit **5** to pharmacophore hypothesis 4. Hydrogen bond acceptor (HBA), hydrogen bond donor (HBD), and hydrophobic features (HY1, HY2, and HY3) are mapped to hit **5**. (B) Ligplot diagram showing hydrophobic interaction between aurora A and hit **5**.

Scheme legends

Scheme 1. Flow chart depicting the Ligand Efficiency (LE) based approach for virtual screening of HTS database for aurora kinase inhibitor identification.

Scheme 2. (a) Br₂, AcOH, CH₂Cl₂, 0° C, 8 h, quant.; (b) 2-chlorophenylmagnesium bromide, THF, 0° C, 2 h, 65%; (c) Et₃SiH, TFA, CH₂Cl₂, rt, 1 h, 83%; (d) LiAlH₄, THF, 0° C, 2 h, quant; (e) MnO₂, CH₂Cl₂, MeOH, rt, 8h, 77%; (f) 2-furoyl chloride, Et₃N, CH₂Cl₂, rt, 8 h, 74%; (g) 1 atm H₂, Pd/C, EtOH, rt, 8 h, 95%; (h) EtOH, reflux, 2 h, 52%.

Table 1. Aurora kinase inhibitor hits identified from the HTS database in this study and their features.

Hit	Structure	Aurora A		FQ ^b	PH Rank ^c	PH_FQ Rank ^d
		% inhibition @ 10 μ M	Aurora A IC ₅₀ (μ M) ^a			
1		72.4%	6.40	0.82	308	85
2		78.90%	11.10	0.76	502	214
3		56.50%	11.71	0.82	870	91
4		73.10%	7.27	0.78	206	177
5		81.50%	1.29	0.77	114	193
6		50.20%	7.93	0.78	545	172
7		57.60%	8.35	0.92	443	11

^aValues are expressed as the mean of at least two independent determinations and are within

$\pm 15\%$. ^bFQ – Fit quality of the hit. ^cPH rank – Pharmacophore rank of the hit. ^dPH_FQ rank –

Pharmacophore_Fit quality rank of the hit.

Table 2. Comparison of enrichment factor for the identification of control and new hits from database compounds using PH and PH_FQ screening methods.

Parameter	Control compounds		Database compounds	
	PH	PH_FQ	PH	PH_FQ
	screening	screening	screening	screening
Total number of active molecules identified (hits identified)	54	72	2	7
Total number of molecules selected (no. selected)	223	223	151	151
Total number of active molecules (hits total)	243	243	7	7
Total number of molecules in database (no. Total)	125,243	125,243	125,000	125,000
Enrichment factor (EF) ^a	125	166	237	828

^aEF = (hits identified / no. selected)/ (hits total/ no. total)

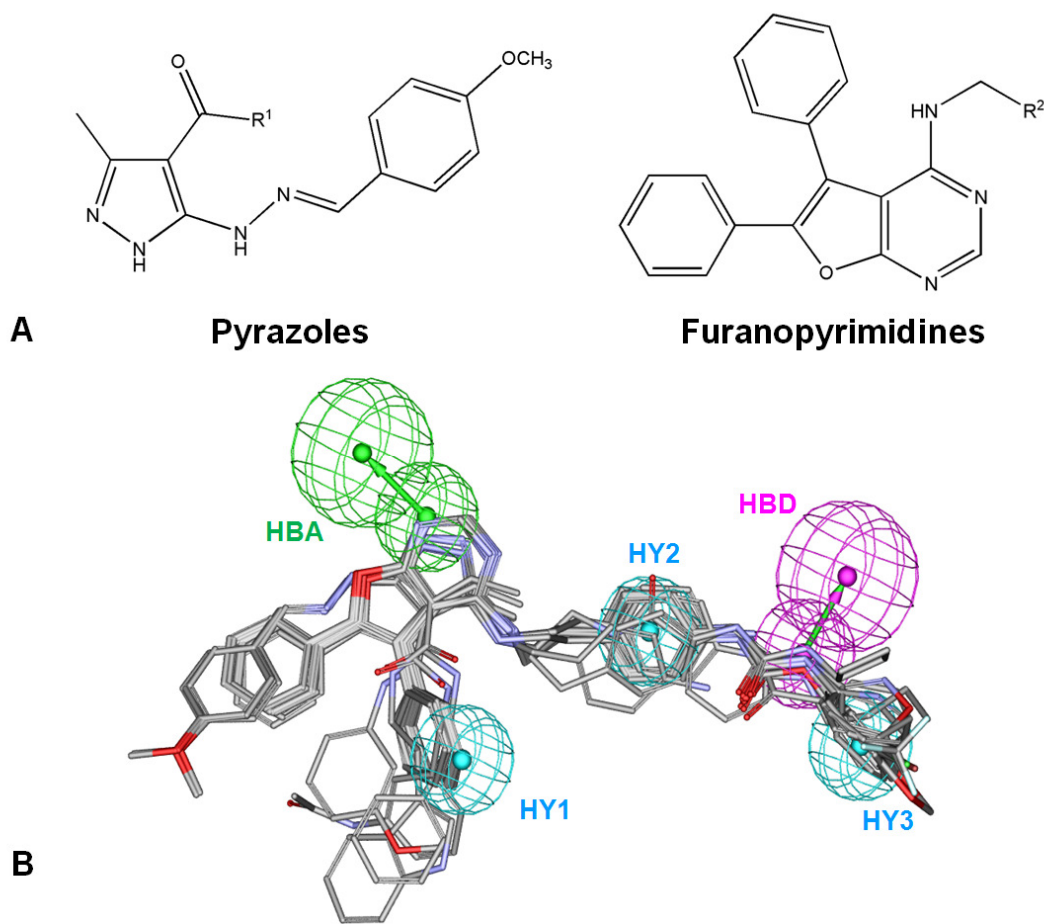


Figure 1. (A) General structures of known aurora kinase inhibitors (pyrazoles and furanopyrimidines) used for constructing the pharmacophore model (see Table S1 and S2, supporting information, for details of training and test sets). (B) Alignment of docked conformations (generated by docking to 2W1C crystal structure) of training set compounds with Hypo 4 model. The model contains five features: one hydrogen bond acceptor (HBA, green spheres), one hydrogen bond donor (HBD, magenta spheres), and three hydrophobic features (HY1, HY2, and HY3, cyan spheres).

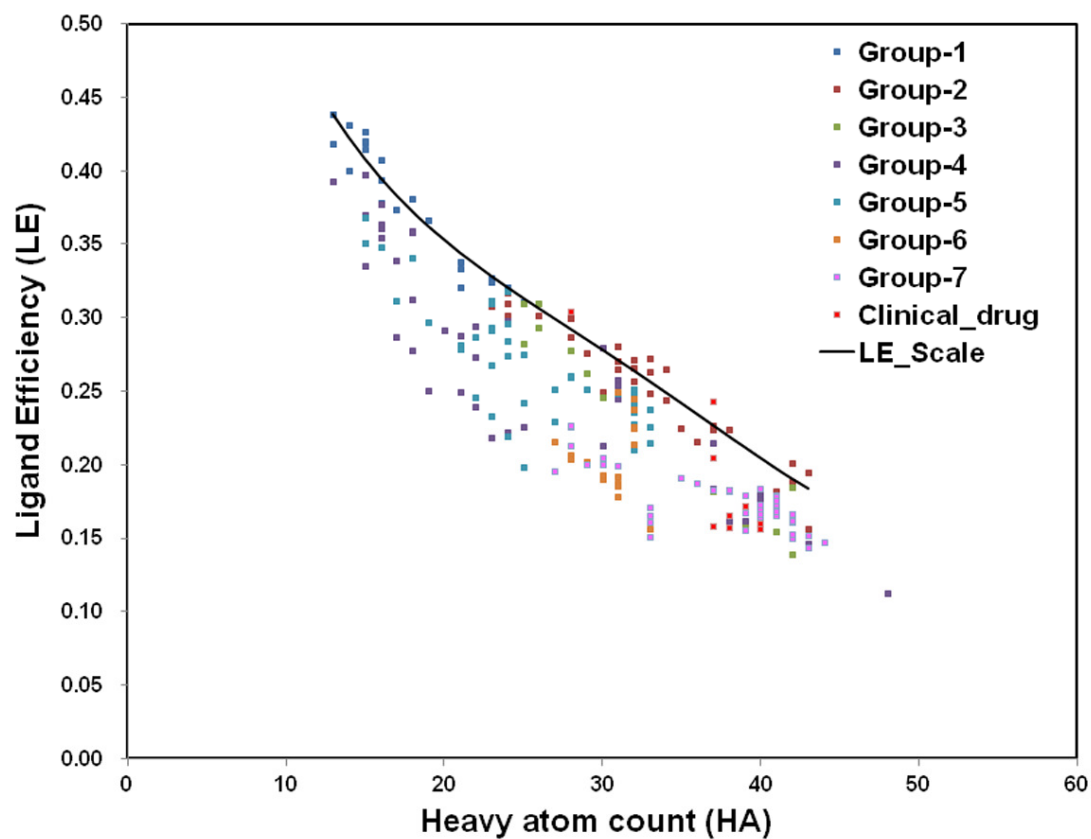


Figure 2. Derivation of LE_Scale function from the plot of ligand efficiency (LE) vs. heavy atom (HA) count of known aurora kinase inhibitors (Group 1–7) and 9 clinical drugs (total 243 control compounds). The LE_Scale function is represented by a black line, which is fitted to the highest LE values over a range of HA count.

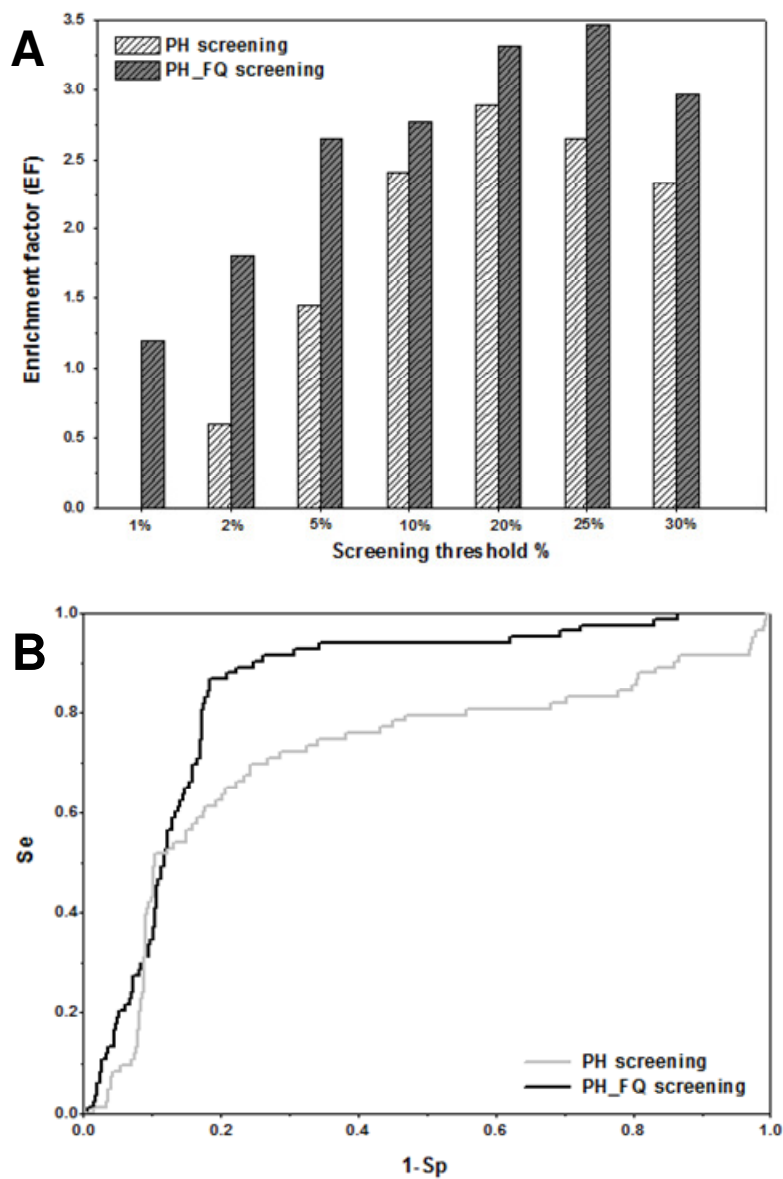


Figure 3. Analysis of control compound retrieval from HTS database. (A) Comparison of enrichment factor (EF) at screening threshold of 1 to 30% for PH and PH_FQ screening methods. (B) Comparison of ROC curve of PH and PH_FQ screening methods.

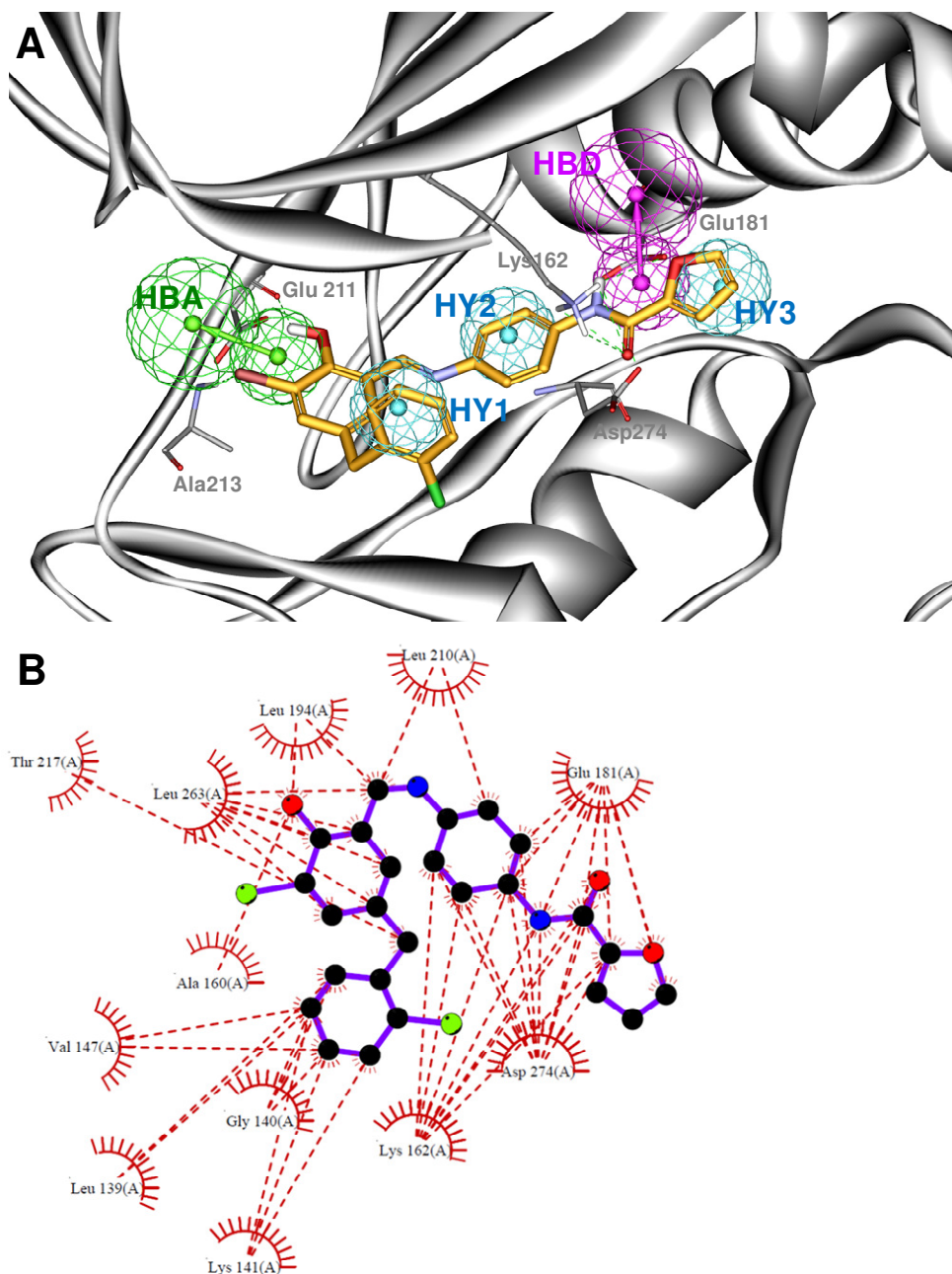
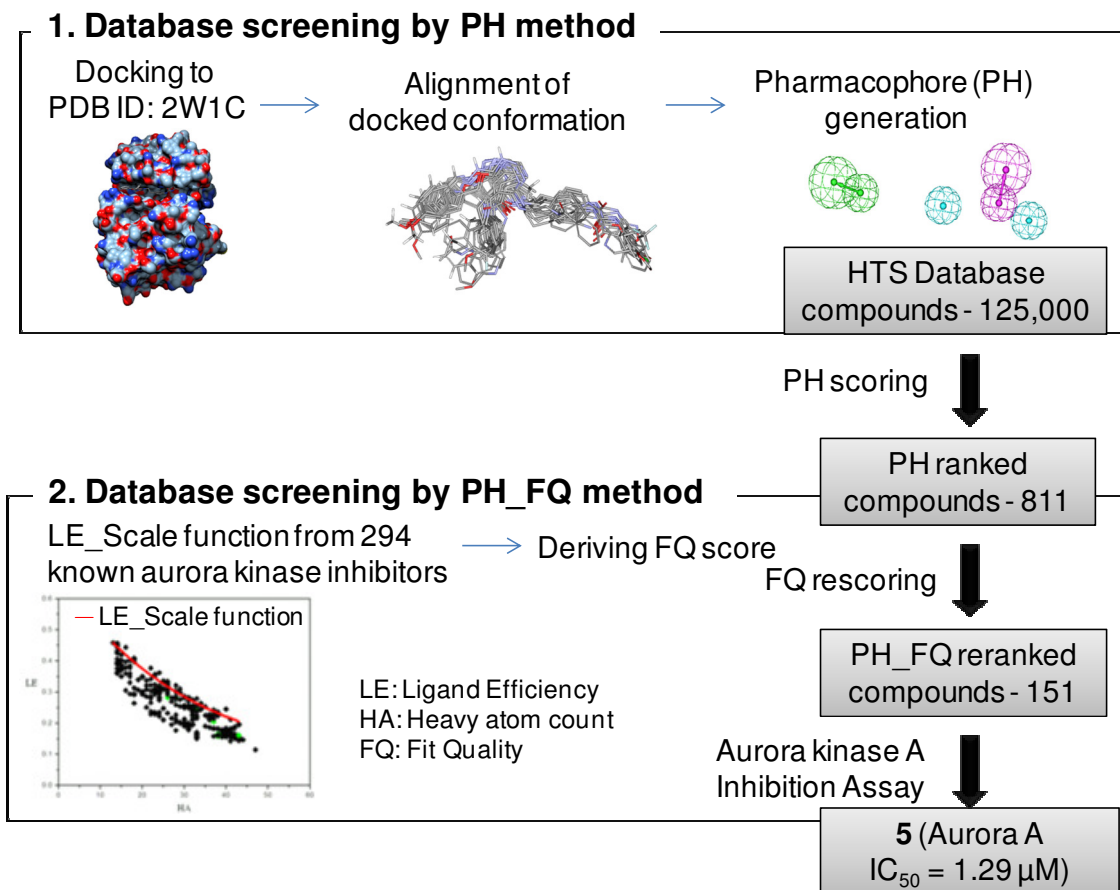
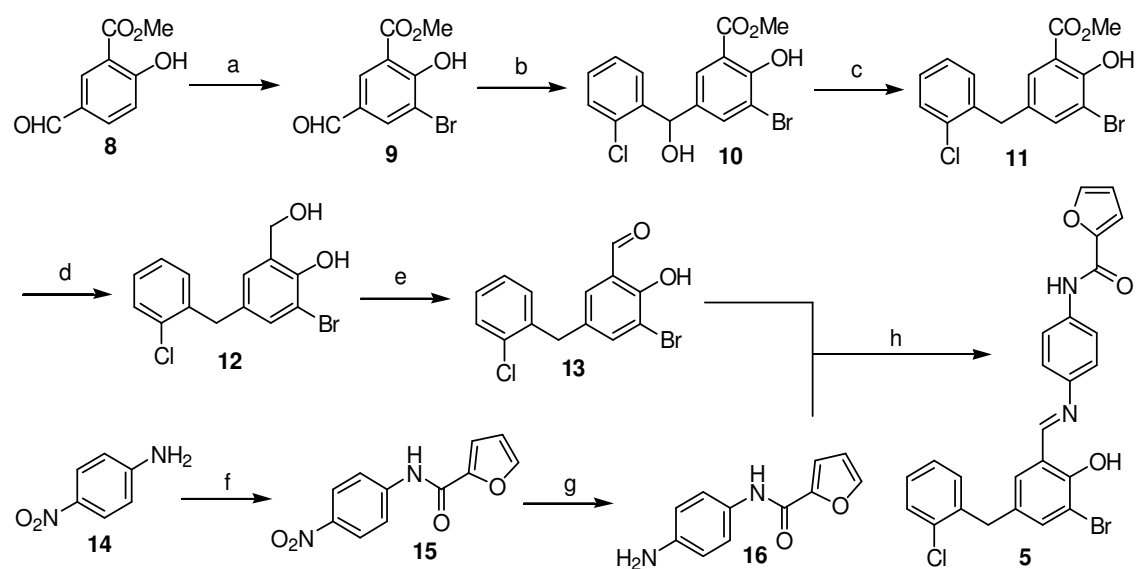


Figure 4. Docking of hit **5** to aurora kinase A (PDB ID: 2W1C). (A) Mapping of docked conformation of hit **5** to pharmacophore hypothesis 4. Hydrogen bond acceptor (HBA), hydrogen bond donor (HBD), and hydrophobic features (HY1, HY2, and HY3) are mapped to hit **5**. (B) Ligplot diagram showing hydrophobic interaction between aurora A and hit **5**.



Scheme 1. Flow chart depicting the Ligand Efficiency (LE) based approach for virtual screening of HTS database for aurora kinase inhibitor identification.



Scheme 2. (a) Br₂, AcOH, CH₂Cl₂, 0° C, 8 h, quant.; (b) 2-chlorophenylmagnesium bromide, THF, 0° C, 2 h, 65%; (c) Et₃SiH, TFA, CH₂Cl₂, rt, 1 h, 83%; (d) LiAlH₄, THF, 0° C, 2 h, quant; (e) MnO₂, CH₂Cl₂, MeOH, rt, 8h, 77%; (f) 2-furoyl chloride, Et₃N, CH₂Cl₂, rt, 8 h, 74%; (g) 1 atm H₂, Pd/C, EtOH, rt, 8 h, 95%; (h) EtOH, reflux, 2 h, 52%.